

Pyrazine and 1,4-Diazabicyclo[2.2.2]octane as Magnetic Exchange Propagating Bridges in Binuclear Copper(II) and Vanadyl Complexes

Muin S. Haddad,¹ David N. Hendrickson,^{*2} J. Patrick Cannady, Russell S. Drago, and David S. Bieksza

Contribution from the School of Chemical Sciences, University of Illinois, Urbana, Illinois 61801. Received June 12, 1978

Abstract: The preparation and magnetic properties are reported for $[\text{Cu}_2(\text{tren})_2(\text{bridge})](\text{ClO}_4)_4$, where the bridge is either pyrazine (pyz) or 1,4-diazabicyclo[2.2.2]octane (Dabco), and $[\text{Cu}_2(\text{tren})_2(\text{bridge})](\text{BPh}_4)_4$, where the bridge is either 4,4'-bipyridine (4,4'-bpy) or 1,2-bis(4-pyridyl)ethylene (BPE). Only the pyrazine complex shows signs of an antiferromagnetic exchange interaction in magnetic susceptibility data taken down to 4.2 K. In this complex, the interaction is weak with $J = -3.2 \text{ cm}^{-1}$, in spite of the fact that the two $\text{Cu}(\text{tren})^{2+}$ units have their d_{z^2} orbitals in which the unpaired electrons reside pointing directly into the nitrogen lone-pair orbitals of the pyrazine. The Cu-tren-BPE complex does show evidence of a very weak ($0.02 \text{ cm}^{-1} < |J| < \sim 0.5 \text{ cm}^{-1}$) exchange interaction with the appearance of a seven-line copper hyperfine pattern in its Q-band EPR spectrum. The magnetic susceptibility vs. temperature curve for the potentially polymeric compound $[\text{Cu}(\text{pyz})_2](\text{ClO}_4)_2$ shows a maximum at 12.1 K. The complex $[\text{VO}(\text{hfac})_2]_2\text{B}$ with $\text{B} = \text{Dabco}$ does not show any signs of an exchange interaction in magnetism data taken to 4.2 K, but when B is either pyz, 2-Me-pyz, or 2,5-Me₂-pyz, there is a maximum in the susceptibility vs. temperature curves at 31.5, 12.1, and 7.0 K, respectively. The data for these last three binuclear vanadyl complexes were fit to give $J = -19, -6.7, \text{ and } -4.0 \text{ cm}^{-1}$. It is suggested that the pyrazine bridges in these vanadyl complexes are bridging between equatorial sites. From the work on the copper(II) and vanadyl complexes, it is concluded that pyrazine (or Dabco) is not a very good bridge for propagating an exchange interaction between two metal ions with σ ground states, or, for that matter, between two metal ions with π ground states. The formation constants K_1 and K_2 for binding to pyrazine one or two $\text{VO}(\text{hfac})_2$ complexes to form $\text{VO}(\text{hfac})\cdot\text{pyz}$ or $[\text{VO}(\text{hfac})]_2\cdot\text{pyz}$ were determined to be $K_1 \approx 1.5 \times 10^6 \text{ M}^{-1}$ and $K_2 \approx 2.0 \times 10^3 \text{ M}^{-1}$, respectively.

Introduction

In the last few years, pyrazine (pyz), acting as a bridge in binuclear transition-metal complexes, has attracted the interest of several workers. The basic question under study is the effectiveness of pyrazine in propagating an interaction between two transition-metal complexes. In 1969, Creutz and Taube first reported³ on the mixed-valence species $[(\text{NH}_3)_5\text{Ru-pyz-Ru}(\text{NH}_3)_5]^{5+}$. There has been considerable controversy in the literature about the rate of thermal electron transfer for this species. Very recent work⁴ has shown that the unpaired electron is localized in a (d_{xz}, d_{yz}) orbital on the Ru(III) center and is transferred through the pyrazine bridge at a rate which is fast on the ¹H NMR time scale but slow on the EPR time scale. There was also no evidence of a magnetic exchange interaction in the magnetic susceptibility data taken down to 4.2 K for a salt of the binuclear Ru(III) species $[(\text{NH}_3)_5\text{Ru-pyz-Ru}(\text{NH}_3)_5]^{6+}$.

Hatfield and co-workers have studied the magnetism of two polymeric copper(II) complexes that have pyrazine bridges. No superexchange interaction was observed for $[\text{Cu}(\text{hfac})_2(\text{pyz})]_x$, where hfac^- is hexafluoroacetylacetonate, with susceptibility data taken down to 1.8 K.⁵ X-ray diffraction work⁶ has shown that the linear-chain structure of this compound results from pyrazine bridging in the axial (i.e., z axis) direction between square-planar $\text{Cu}(\text{hfac})_2$ units. The absence of any exchange interaction was attributed to the fact that the plane of the pyrazine bridge lies in the xz plane of the $\text{Cu}(\text{hfac})_2$ unit. The copper(II) ground state is $d_{x^2-y^2}$ and there is no effective π -orbital pathway available on the pyrazine. In this same work,⁵ no exchange interaction was detected for polymeric $[\text{Cu}(\text{hfac})_2(\text{Dabco})]_x$, where Dabco is 1,4-diazabicyclo[2.2.2]octane, a bridge affording only a σ type of exchange pathway.



On the other hand, an antiferromagnetic interaction (exchange parameter, $J = -7.4 \pm 0.1 \text{ cm}^{-1}$) was noted for $[\text{Cu}(\text{NO}_3)_2(\text{pyz})]_x$.⁷ In this compound, the pyrazine groups lie canted some 50° out of the copper xy plane. This allows for $d_{x^2-y^2}-\pi(\text{b}_1\text{g})$ overlap which was interpreted to lead to a π -orbital pathway for the pyrazine superexchange interactions.

In a recent paper,⁸ Hoffmann and co-workers employed the extended Hückel molecular orbital approach to analyze the magnetic exchange interactions seen for several binuclear copper(II) complexes. Pyrazine and Dabco bridges were considered and it was concluded that these two bridges would be very effective in supporting antiferromagnetic interactions with a σ type of exchange pathway. The two nitrogen lone electron pairs on either pyz or Dabco interact via empty and occupied σ levels to produce an appreciable splitting in the lone-pair energy levels. It was suggested that this through-bond coupling would provide an effective σ type of exchange pathway. The binuclear copper(II) complex should be constructed so that the copper(II) ions have their unpaired electrons in σ -type orbitals interacting directly with the nitrogen lone-pair orbitals of pyrazine (Dabco). In this paper, we report the preparation and magnetic properties of binuclear metal complexes which allow a determination of the various delocalization pathways for these bridging ligands. Pyrazine and Dabco have been incorporated as bridges between two trigonal-bipyramidal $\text{Cu}(\text{tren})^{2+}$ units (tren is 2,2',2''-tri-aminotriethylamine). The copper(II) unpaired electrons are located in d_{z^2} orbitals which are directed at the nitrogen lone-pair orbitals. Pyrazine has been incorporated as a bridging ligand between two $\text{Cu}(\text{hfac})_2$ moieties and two $\text{VO}(\text{hfac})_2$ units have been bridged by pyz, a substituted pyz, and Dabco.

Experimental Section

Compound Preparation. The ligands 2,2',2''-tri-aminotriethylamine (Ames Laboratory, Inc.), 1,1,1,5,5,5-hexafluoroacetylacetonate, acetylacetonate (Columbia Organic Chemicals), pyrazine, 2-methylpy-

razine, 2,5-dimethylpyrazine, 4,4'-dipyridyl dihydrate, 1,2-bis(4-pyridyl)ethylene, and 1,4-diazabicyclo[2.2.2]octane (Aldrich) were used as received. All other materials were of reagent grade quality. Elemental analyses were performed by the Microanalytical Laboratory of the School of Chemical Sciences, University of Illinois.

[Cu₂(tren)₂(pyz)](ClO₄)₄. To an aqueous solution (20 mL) of ca. 1.0 g (4 mmol) of CuSO₄·5H₂O were added ca. 0.6 mL of 2,2',2''-triaminotriethylamine (tren) followed by an aqueous solution (5 mL) of ca. 0.16 g (2 mmol) of pyrazine (pyz). The solution was filtered and an aqueous solution containing an excess (up to eightfold) of NaClO₄ was added to effect precipitation of a microcrystalline, blue solid. Sometimes the compound precipitates as a hydrate. Anal. Calcd for C₁₆H₄₀N₁₀Cu₂Cl₄O₁₆: C, 21.42; H, 4.46; N, 15.61; Cu, 14.17. Found: C, 21.23; H, 4.31; N, 15.49; Cu, 14.47.

[Cu₂(tren)₂(4,4'-bpy)](BPh₄)₄. To an aqueous solution (100 mL) of ca. 1.0 g (4 mmol) of CuSO₄·5H₂O was added ca. 0.6 mL of tren, followed by a 6:1 H₂O/EtOH solution (70 mL) of ca. 0.25 g (1.3 mmol) of 4,4'-bipyridine dihydrate (4,4'-bpy·2H₂O). To the dark blue filtered solution was added an aqueous solution of ca. 0.50 g of NaBPh₄. The resulting green solid was collected, washed with ethanol, then diethyl ether, and dried in a vacuum desiccator over P₂O₁₀. Anal. Calcd for C₁₁₈H₁₂₄N₁₀Cu₂B₄: C, 76.50; H, 6.75; N, 7.56; Cu, 6.86. Found: C, 76.22; H, 6.49; N, 7.41; Cu, 6.88.

[Cu₂(tren)₂(BPE)](BPh₄)₄. To prepare this compound reproducibly, it was found necessary to carry out the preparation by metathesis of [Cu₂(tren)₂(BPE)](ClO₄)₄. The latter is prepared in the following way. To an aqueous solution (20 mL) of ca. 1.6 g of Cu(ClO₄)₂·6H₂O was added ca. 0.6 mL of tren. To the filtered solution a filtered ethanolic solution (20 mL) of ca. 0.25 g of 1,2-bis(4-pyridyl)ethylene (BPE) was added. Immediate precipitation of a blue solid occurred. To a 3:1 MeOH/H₂O solution (280 mL) of ca. 0.83 g (4.4 mmol) of [Cu₂(tren)₂(BPE)](ClO₄)₄ a methanol solution (50 mL) of ca. 0.78 g (2.3 mmol) of NaBPh₄ was added to effect the precipitation of a light green product. The solid was collected, washed with diethyl ether, and then dried in vacuo over P₂O₁₀. Anal. Calcd for C₁₂₀H₁₂₆N₁₀Cu₂B₄: C, 76.76; H, 6.71; N, 7.46; Cu, 6.77. Found: C, 76.49; H, 6.59; N, 7.42; Cu, 6.73.

[Cu(py₂)₂](ClO₄)₂. This compound was prepared according to the reported procedure.⁹ However, it was found that, in order to effect precipitation, minimum volumes of water should be used. In a typical preparation, ca. 1.50 g (4 mmol) of Cu(ClO₄)₂·6H₂O was dissolved in 5 mL of water. An aqueous solution (5 mL) of ca. 0.64 g (8 mmol) of pyrazine was then added. The solution color darkened and then "gelled". Filtration separated a blue solid with a lavender tint. The complex was washed with ethanol and dried in vacuo over P₂O₁₀. Anal. Calcd for C₈H₈N₄CuCl₂O₈: C, 22.74; H, 1.89; N, 13.25; Cu, 15.04. Found: C, 22.92; H, 1.90; N, 12.94; Cu, 15.17.

[Cu₂(tren)₂(Dabco)](ClO₄)₄. To an aqueous solution (30 mL) of ca. 0.74 g (2 mmol) of Cu(ClO₄)₂·6H₂O were added ca. 0.3 mL of tren followed by an aqueous solution (10 mL) of ca. 0.34 g (3 mmol) of Dabco. To the filtered solution, an aqueous solution (10 mL) of ca. 1.01 g (8 mmol) of NaClO₄ was added. Evaporation of the solution down to ca. 40 mL resulted in the formation of a blue solid. Anal. Calcd for C₁₈H₄₈N₁₀Cu₂Cl₄O₁₆: C, 23.25; H, 5.22; N, 15.07; Cu, 13.67. Found: C, 23.17; H, 5.10; Cu, 13.90; N, 15.01.

VO(hfac)₂·H₂O, where hfac is 1,1,1,5,5,5-hexafluoroacetylacetonate, was prepared by literature methods¹⁰ and recrystallized three times from benzene under an argon blanket to produce the anhydrous material.

[VO(hfac)₂]₂B, where B is pyz, 2-Me-pyz, 2,5-Me₂-pyz, or Dabco, was prepared by adding 1 equiv of B to a hot benzene or chloroform solution containing 2 equiv of VO(hfac)₂. The polycrystalline product precipitated either immediately or after cooling to room temperature. Anal. Calcd for C₂₄H₈N₂V₂F₂₄O₁₀: C, 27.70; H, 0.78; N, 2.69; V, 9.75. Found: C, 27.46; H, 0.78; N, 2.59; V, 9.70. Calcd for C₂₅H₁₀N₂V₂F₂₄O₁₀: C, 28.43; H, 0.95; N, 2.65; V, 9.65. Found: C, 28.47; H, 0.96; N, 2.77; V, 10.07. Calcd for C₂₆H₁₂N₂V₂F₂₄O₁₀: C, 29.18; H, 1.13; N, 2.62; V, 9.52. Found: C, 29.13; H, 1.06; N, 2.50; V, 9.68. Calcd for C₂₆H₁₆N₂V₂F₂₄O₁₀: C, 29.07; H, 1.50; N, 2.61; V, 9.48. Found: C, 28.86; H, 1.49; N, 2.52; V, 9.73.

VO(acac)₂ was prepared according to a literature procedure.¹¹ [VO(acac)₂]₂(BPE), where acac is acetylacetonate, was prepared by adding a chloroform solution (12 mL) of ca. 0.17 g (1 mmol) of BPE to a chloroform solution (50 mL) of ca. 0.49 g (2 mmol) of VO(acac)₂. The resulting dark green solution was filtered and petroleum ether (bp 90–110 °C) was added to effect precipitation of the brown-yellow

product. Anal. Calcd for C₃₂H₃₈N₂V₂O₁₀: C, 53.96; H, 5.34; N, 3.93; V, 14.34. Found: C, 53.75; H, 5.26; N, 3.92; V, 14.04.

[Cu(hfac)₂]₂B, where B is pyz or Dabco, was prepared according to literature methods.^{6,12} Anal. Calcd for C₂₄H₈N₂Cu₂F₂₄O₈: C, 27.84; H, 0.78; N, 2.71; Cu, 12.27. Found: C, 27.80; H, 0.80; N, 2.90; Cu, 12.33. Calcd for C₂₆H₁₆N₂Cu₂F₂₄O₈: C, 29.26; H, 1.50; N, 2.62; Cu, 11.91. Found: C, 29.24; H, 1.41; N, 2.60; Cu, 12.21.

Spectrophotometric Formation Constant Determination. Studies were carried out in methylene chloride which had been refluxed over and then distilled from calcium hydride under a dry nitrogen atmosphere. Electronic absorption spectra were recorded on a Cary-14A spectrophotometer and analyzed at two wavelengths using a least-squares fitting routine described elsewhere.¹³ Spectra were obtained at room temperature (23 °C).

Physical Measurements. Variable-temperature (4.2–286 K) magnetic susceptibility data were obtained using a Princeton Applied Research Model 150A vibrating-sample magnetometer operating at 12.7 kG and calibrated with CuSO₄·5H₂O as described in a previous paper.¹⁴ All data were corrected for diamagnetism¹⁵ and TIP (taken as 120 × 10⁻⁶ cgsu per binuclear complex). All least-squares fittings were performed using a new version of the minimization computer program STEPT.¹⁶

EPR spectra of powdered samples, as well as glasses, were recorded on a Varian E-9 X-band spectrometer and a Varian E-15 Q-band spectrometer as described previously.¹⁷

X-ray powder patterns were obtained with a Norelco (Phillips Electronics Co.) powder diffractometer employing a Cu K α X-ray source. The samples were prepared by grinding the solid and filling a cavity in an aluminum sample holder. Scan rates of 1° of 2 θ per min were used.

The molecular orbital calculations were performed using the CNDO/2 method.¹⁸ The sources of the molecular dimensions will be mentioned in the Exchange Mechanism section.

Results

Magnetic Susceptibility. Variable-temperature (4.2–286 K) magnetic susceptibility data were collected for 11 of the 12 complexes prepared in this study. The data are given in Tables I–XI.¹⁹ Four Cu(II) and two VO²⁺ compounds did not show any signs of a magnetic exchange in the susceptibility data taken down to ca. 4.2 K; these compounds are [Cu₂(tren)₂(4,4'-bpy)](BPh₄)₄ where 4,4'-bpy is 4,4'-bipyridine, [Cu₂(tren)₂(BPE)](BPh₄)₄ where BPE is 1,2-bis(4-pyridyl)ethylene, [Cu₂(tren)₂(Dabco)](ClO₄)₄, [Cu(hfac)₂]₂(pyz), [VO(hfac)₂]₂(Dabco), and [VO(acac)₂]₂(BPE). Figure 1 illustrates the effective magnetic moment vs. temperature curves for [Cu₂(tren)₂(Dabco)](ClO₄)₄ and [VO(hfac)₂]₂(Dabco). Data were not collected for [Cu(hfac)₂]₂(Dabco).

The susceptibility data for [VO(hfac)₂]₂B, where B is pyz, 2-Me-pyz, or 2,5-Me₂-pyz, and [Cu₂(tren)₂(pyz)](ClO₄)₄ were least squares fit to the Bleaney-Bowers equation²⁰ for isotropic exchange in a copper(II) dimer:

$$\chi_M = \frac{Ng^2\beta^2}{kT} \left[\frac{2}{3 + \exp(-2J/kT)} \right] + N\alpha \quad (1)$$

For the compound [Cu(py₂)₂](ClO₄)₂ the data were least squares fit to eq 1 as well as to the following equation for a Cu(II) tetramer with D_{4h} symmetry.

$$\chi_M = \frac{Ng^2\beta^2}{kT} \left[\frac{18e^x + 30e^{-3x}}{2e^{3x} + 9e^x + 5e^{-3x}} \right] + N\alpha \quad (2)$$

In eq 2, x is equal to $-2J/3kT$. The derivation of eq 2 was carried out as per a standard procedure.²¹ In both of the above equations the symbols have their usual meaning. However, two points must be clarified. First, χ_M in eq 1 or 2 is the corrected molar paramagnetism of an exchange interacting binuclear unit or tetrameric unit, respectively. Second, $N\alpha$ is taken as 120 × 10⁻⁶ cgsu per mol of binuclear unit in eq 1, whereas it is taken as 240 × 10⁻⁶ cgsu per tetrameric unit in eq 2.

Two different approaches were tried in fitting the data for each compound. On the one hand, g was held fixed and J was

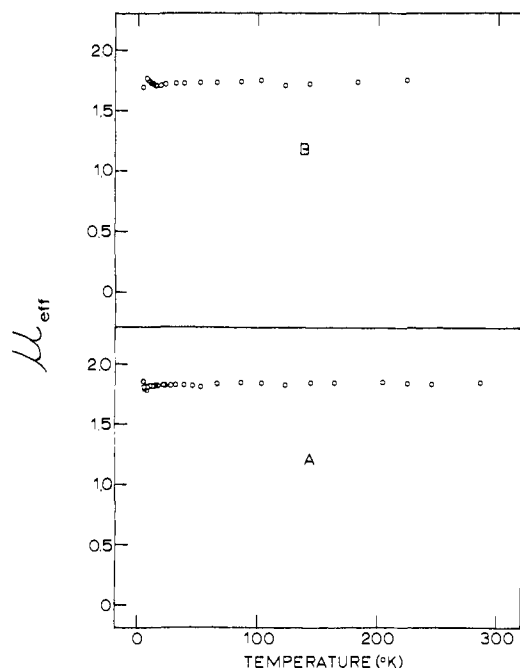


Figure 1. The effective magnetic moment vs. temperature curves for $[\text{Cu}_2(\text{tren})_2(\text{Dabco})](\text{ClO}_4)_4$ (lower curve) and $[\text{VO}(\text{hfac})_2]_2(\text{Dabco})$ (upper curve).

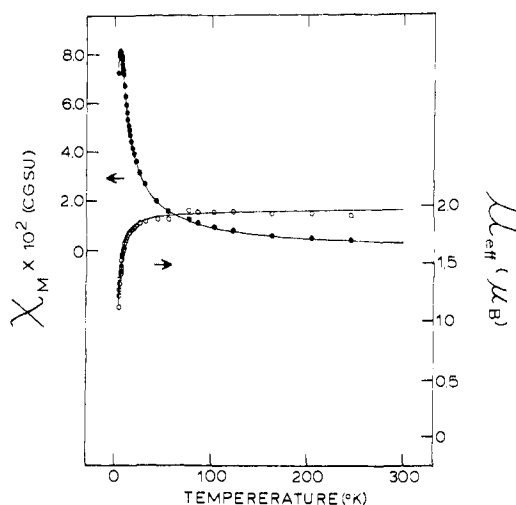


Figure 2. Molar paramagnetic susceptibility, χ_M , per binuclear complex and effective magnetic moment, μ_{eff} , per Cu(II) ion vs. temperature curves for a solid sample of $[\text{Cu}_2(\text{tren})_2(\text{py}_2)](\text{ClO}_4)_4$. The solid lines result from a least-squares fit to the theoretical equation.

varied as the only parameter. On the other hand, both g and J were varied to least squares fit the data. The quality of the fit can be gauged by the standard error (SE).²²

$$\text{SE} = \sum_{i=1}^{\text{NP}} [\mu_{\text{eff}}(\text{obsd})_i - \mu_{\text{eff}}(\text{calcd})_i]^2 / (\text{NP} - k)]^{1/2} \quad (3)$$

In eq 3, k is the number of variable parameters used to fit the NP data points.

The magnetic susceptibility data for $[\text{Cu}_2(\text{tren})_2(\text{py}_2)](\text{ClO}_4)_4$ run from 285.5 K, where $\mu_{\text{eff}}/\text{Cu}$ is $1.85 \mu_B$, to 4.2 K where $\mu_{\text{eff}}/\text{Cu}$ is $1.13 \mu_B$. An antiferromagnetic interaction is present in this compound with a maximum in the susceptibility vs. temperature curve at ca. 7.0 K. Least-squares fitting the data to eq 1 with J and g as parameters yields $J = -3.2 \text{ cm}^{-1}$ and $g = 2.222$. The experimental and calculated curves are shown in Figure 2.

The corrected molar magnetic susceptibility vs. temperature curves for $[\text{VO}(\text{hfac})_2]_2(\text{py}_2)$, $[\text{VO}(\text{hfac})_2]_2(2\text{-Me-pyz})$, and

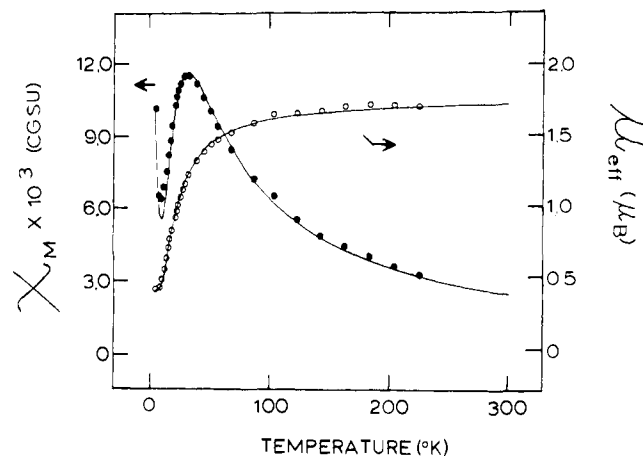


Figure 3. Molar paramagnetic susceptibility vs. temperature and effective magnetic moment vs. temperature curves for $[\text{VO}(\text{hfac})_2]_2(\text{py}_2)$. Solid lines represent the fit to the theoretical equation.

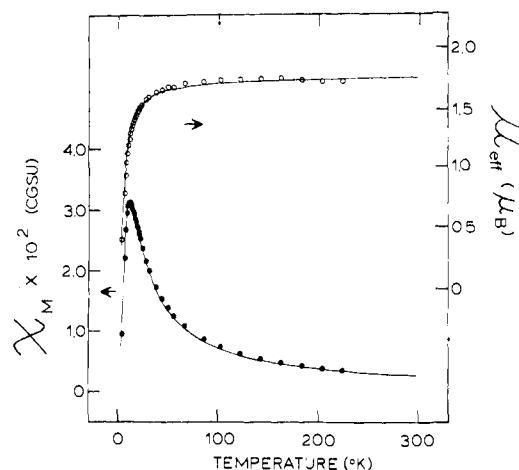


Figure 4. Molar paramagnetic susceptibility vs. temperature and effective magnetic moment vs. temperature curves for $[\text{VO}(\text{hfac})_2]_2(2\text{-Me-pyz})$. Solid lines represent the fit to the theoretical equation.

$[\text{VO}(\text{hfac})_2]_2(2,5\text{-Me}_2\text{-pyz})$ are also indicative of antiferromagnetic interactions with susceptibility maxima at 31.5, 12.1, and 7.0 K, respectively. Figures 3, 4, and 5, respectively, illustrate the experimental data, as well as the calculated curves obtained from least-squares fitting to eq 1. In all three cases, the fitting was carried out with J and g as parameters. For the compound $[\text{VO}(\text{hfac})_2]_2\text{pyz}$, a parameter PAR ($4.2/T$) was added to eq 1 to account for the monomeric impurities contribution to the susceptibility. PAR was fixed at 0.01 cgsu (χ_M at 4.2 K). The resulting J values are -19 , -6.7 , and -4.0 cm^{-1} , respectively. For the pyz compound, $g = 1.917$ is obtained, while for the 2-Me-pyz and 2,5-Me₂-pyz compounds g values of 1.992 and 1.927 were obtained, respectively.

The corrected magnetic susceptibility data for $[\text{Cu}(\text{pyz})_2](\text{ClO}_4)_2$ are indicative of the presence of an antiferromagnetic interaction with a χ_M vs. T maximum at 12.1 K. Because the structure of this compound is uncertain, the data were least squares fit to both eq 1 for a Cu(II) dimer and to eq 2 for a Cu(II) tetramer with D_{4h} symmetry. In both cases, J was varied and g was held constant at 2.06. Figure 6 illustrates the experimental and calculated curves. The broken lines are the calculated curves resulting from the fit to the dimer eq 1, while the solid lines represent the fit to eq 2. The standard error SE for the dimer fitting is 0.13 while SE for the fitting is 0.039. The J values obtained from both fittings are $J(\text{dimer}) = -10.8 \text{ cm}^{-1}$ and $J(\text{tetramer}) = -10.1 \text{ cm}^{-1}$.

Electron Paramagnetic Resonance. The Q-band EPR

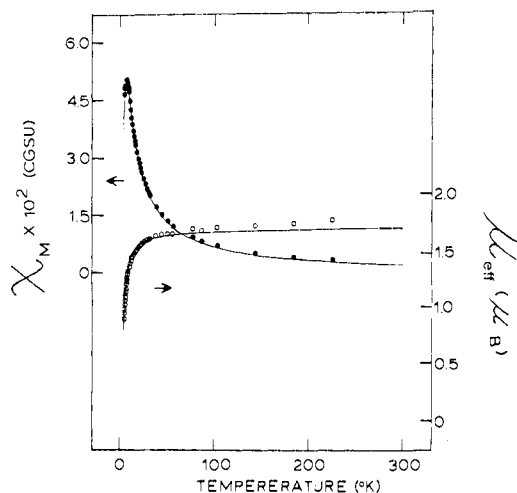


Figure 5. Molar paramagnetic susceptibility vs. temperature and effective magnetic moment vs. temperature curves for [VO(hfac)₂]₂(2,5-Me₂-pyz). Solid lines represent the fit to the theoretical equation.

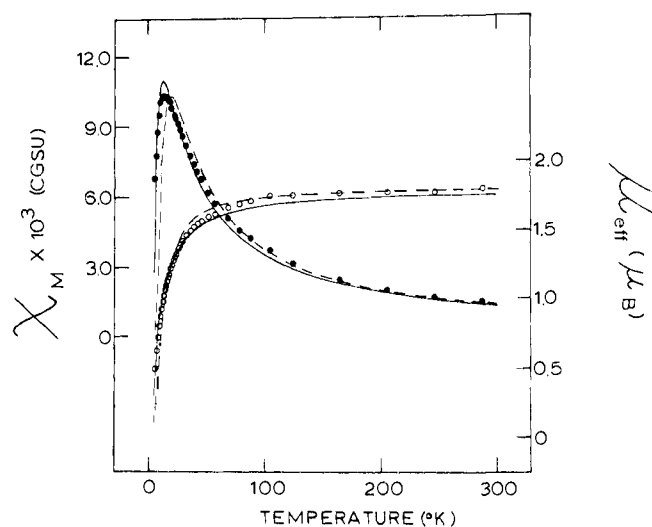


Figure 6. Molar paramagnetic susceptibility and effective magnetic moment vs. temperature data for [Cu(pyz)₂](ClO₄)₂.

spectra of [Cu₂(tren)₂(L)](ClO₄)₄, where L = pyz or Dabco, and [Cu₂(tren)₂(L')](BPh₄)₄, where L' = 4,4'-bpy or BPE, indicate a trigonal-bipyramidal coordination geometry about each Cu(II) ion in that g_{||} is close to the free electron g value. In all cases, there is no appreciable change in the spectrum in changing the sample temperature from room temperature to ca. 80 K.

The Q-band spectrum of [Cu₂(tren)₂(pyz)](ClO₄)₄ exhibits three signals with g₁ = 2.191, g₂ = 2.158, and g₃(g_{||}) = 2.004. The X-band spectrum exhibits a weak ΔM_s = 2 transition at ca. 1500 G and two ΔM_s = 1 transitions with g₁(g_⊥) = 2.203 and g₂(g_{||}) = 2.017. Both the Q-band and the X-band spectra of [Cu₂(tren)₂(Dabco)](ClO₄)₄ are axial with g_⊥ = 2.163 and g_{||} = 2.017 in the Q-band spectrum and with g_⊥ = 2.146 and g_{||} = 2.017 in the X-band spectrum. The Q-band spectrum of [Cu₂(tren)₂(4,4'-bpy)](BPh₄)₄ exhibits a broad g_⊥ = 2.157 signal and a g_{||} = 2.017 signal, while the X-band for this same compound shows three g values as g₁ = 2.239, g₂ = 2.125, and g₃(g_{||}) = 2.030.

Interestingly, the Q-band spectrum of the compound [Cu₂(tren)₂(BPE)](BPh₄)₄ is rhombic with a seven-line copper hyperfine pattern on the lowest field g₁ signal, as indicated in Figure 7. The three g values for the signals in this spectrum are g₁ = 2.203, g₂ = 2.126, and g₃(g_{||}) = 2.009. The interline

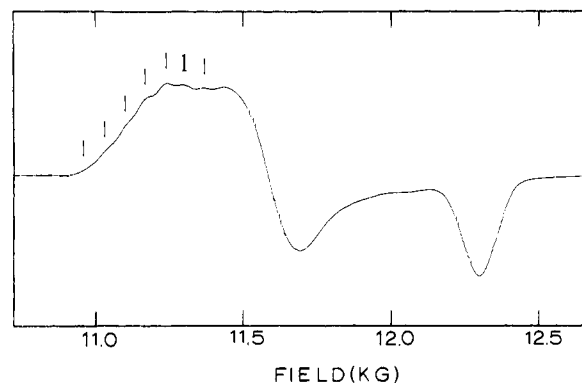


Figure 7. Q-Band EPR spectrum of a powdered sample of [Cu₂(tren)₂(BPE)](BPh₄)₄.

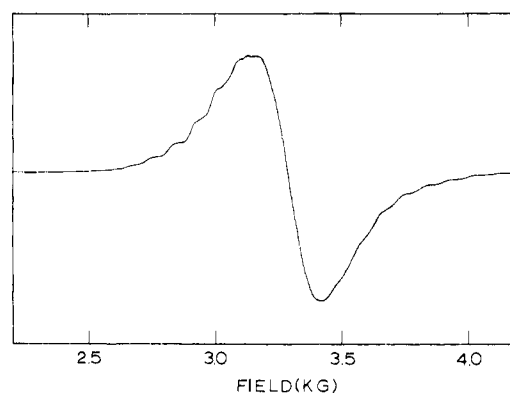


Figure 8. The 10 K X-band EPR spectrum of a powdered sample of [VO(hfac)₂]₂(2,5-Me₂-pyz).

spacings of the seven-line hyperfine pattern on the g₁ signal range from 64 to 70 G with an average of 68 G. The X-band spectrum shows a single derivative around g = 2.107 with a few copper hyperfine lines resolved on the low-field part of the derivative signal.

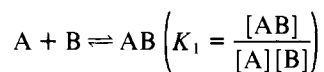
Both the Q-band and the X-band spectra of [Cu(pyz)₂](ClO₄)₂ are very typical of a square-planar Cu(II) coordination geometry, with a relatively sharp derivative signal at g = 2.061 and a weak g = 2.275 signal.

The X-band spectra of powdered solids of [VO(hfac)₂]₂B, where B is pyz, 2-Me-pyz, 2,5-Me₂pyz, or Dabco, and [VO(acac)₂]₂BPE show single derivatives in the ΔM_s = 1 region at g = 2.00. All of the vanadyl compounds, except the Dabco compound, show a ΔM_s = 2 transition at ca. 1400 G. There is no change in the g value on changing the sample temperature from room temperature (293 K) to 10 K; however, for the 2-Me-pyz and 2,5-Me₂-pyz compounds, vanadium hyperfine is resolved in the low-temperature spectra. Both of these compounds show a 15-line vanadium hyperfine pattern impressed on the g_{||} signal; see Figure 8. In these 15-line patterns, the average interline spacings are 79 and 85 G, respectively. These values are approximately one-half of the A_{||}(V) value for a monomeric vanadyl complex as would be expected. The two unpaired electrons in each of these binuclear complexes are exchanging between the two vanadyl centers rapidly on the EPR time scale and the hyperfine interaction with two equivalent vanadium(IV) ions (I = 7/2) leads to a 15-line pattern. Liquid-nitrogen temperature, toluene-CH₂Cl₂ or toluene-CHCl₃ glass spectra were run for these binuclear vanadyl complexes; the spectra clearly indicated that the binuclear complexes dissociate in solution. Eight-line vanadium hyperfine patterns were seen with A(av) = ca. 100 G.

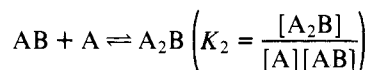
Single derivatives were seen in the ΔM_s = 1 region of the X-band spectra of [Cu(hfac)₂]₂B, where B is either pyz or

Dabco. Both signals occurred at $g = 2.14$. Half-field $\Delta M_s = 2$ signals at ca. 1500 G were seen for both compounds.

Solution Formation Constants for $[\text{VO}(\text{hfac})_2\text{pyz}]$. The formation constants K_1 and K_2 for the equilibria



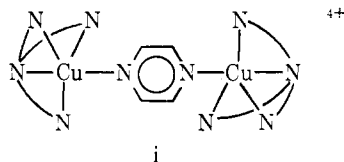
and



where $\text{A} = \text{VO}(\text{hfac})_2$ and $\text{B} = \text{pyrazine}$, were determined by computer fitting spectrophotometric titration data. A series of methylene chloride solutions was prepared in which the concentration of $\text{VO}(\text{hfac})_2$ was $1.96 \times 10^{-3} \text{ M}$ and the concentration of pyrazine varied from zero to $8.00 \times 10^{-3} \text{ M}$. The spectra of these solutions were then recorded in 1-cm quartz cuvettes using pure solvent in the reference beam. An isosbestic point existed for the free $\text{VO}(\text{hfac})_2$ and the 2:1 $\text{VO}(\text{hfac})_2$ to pyrazine adduct. The absorbances of these solutions at wavelengths of 420 and 485 nm were then used to obtain an estimate for the values of the two equilibrium constants. The approximate values were $K_1 \approx 1.5 \times 10^6$, $K_2 \approx 2.0 \times 10^3$. The fit was obtained by allowing K_1 , K_2 , and $\epsilon_{420}(\text{A}_2\text{B})$ to vary while holding $\epsilon_{420}(\text{A})$, $\epsilon_{420}(\text{AB})$, $\epsilon_{480}(\text{A})$, $\epsilon_{480}(\text{AB})$, and $\epsilon_{480}(\text{A}_2\text{B})$ fixed at values determined from the recorded spectra. The $\epsilon_{420}(\text{AB})$ and $\epsilon_{480}(\text{AB})$ values were obtained from limiting values, while $\epsilon_{480}(\text{A}_2\text{B})$ equals $\epsilon_{480}(\text{AB})$ at the isosbestic point. These assumptions are valid for the crude estimates of these constants needed for our purposes.

Discussion

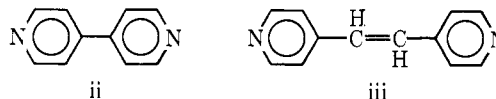
Compound Formulation. One goal of this paper was to construct a binuclear copper(II) complex bridged by either pyz or Dabco which is expected from theory to exhibit an appreciable antiferromagnetic exchange interaction. Hoffmann et al.⁸ suggested that the binuclear complex should be constructed so that the copper(II) orbital in which the unpaired electron resides would be involved in a σ type of interaction with the nitrogen lone-pair orbitals of either the pyz or Dabco bridge. One possibility is to select a copper(II) complex with a d_{z^2} ground state. Two of these d_{z^2} complexes can be bridged by a pyz(Dabco) molecule in the fashion suggested by Hoffmann, viz., i. The tripodal ligand tren (2,2',2''-triaminotriethylamine)



is ideally suited for this purpose. It enforces a trigonal bipyramidal coordination geometry on the copper(II) ion and prevents polymer formation, as has been found in all structural work on compounds involving the $\text{Cu}(\text{tren})^{2+}$ unit.²³⁻²⁶ It was a relatively simple task to prepare $[\text{Cu}_2(\text{tren})_2(\text{pyz})](\text{ClO}_4)_4$ and $[\text{Cu}_2(\text{tren})_2(\text{Dabco})](\text{ClO}_4)_4$. Both of these complexes do exhibit EPR spectra that are indicative of trigonal-bipyramidal Cu(II) coordination geometry (vide supra). The pyz compound also has variable-temperature magnetic susceptibility data that are characteristic of an antiferromagnetic exchange interaction and the data are fit well by the theoretical equation for a copper(II) dimer. It is clear that these two compounds do form binuclear copper(II) cations that are structured in the fashion desired.

The bridges 4,4'-bipyridine (4,4'-bpy) and 1,2-bis(4-pyridyl)ethylene (BPE) are related to pyz and, because they have been investigated as bridges in binuclear mixed-valence $\text{Ru}(\text{NH}_3)_5^{2+/3+}$ complexes,²⁷ it was also of interest to see if

they would be viable bridges to propagate a magnetic exchange interaction. The compounds $[\text{Cu}_2(\text{tren})_2(4,4'\text{-bpy})](\text{BPh}_4)_4$ and $[\text{Cu}_2(\text{tren})_2(\text{BPE})](\text{BPh}_4)_2$ were prepared. Tetraphenylborate salts were prepared because it was anticipated that, owing to the extension of these two bridges, the exchange interaction would be weak and perhaps only detectable by the



observation of copper hyperfine in the EPR spectra. The BPh_4^- ion can provide some degree of magnetic dilution.

The X-ray crystal structure⁶ of $[\text{Cu}(\text{hfac})_2]_2(\text{pyz})$ showed that it is binuclear. It is most reasonable to expect that $[\text{Cu}(\text{hfac})_2]_2(\text{Dabco})$ is isostructural. The good fits of the susceptibility data (vide supra) to the theoretical equation for an exchange interacting $S_1 = S_2 = 1/2$ dimer demonstrate that $[\text{VO}(\text{hfac})_2]_2\text{B}$, where B is variously pyz, 2-Me-Pyz, or 2,5-Me₂-pyz, is also binuclear. The presence of $\Delta M_s = 2$ EPR transitions is also supportive of the binuclear compositions.

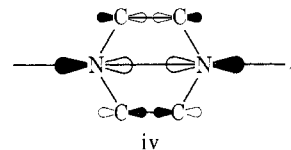
Physical Observables and Magnetic Exchange Mechanisms. The two compounds $[\text{Cu}_2(\text{tren})_2(\text{pyz})](\text{ClO}_4)_4$ and $[\text{Cu}_2(\text{tren})_2(\text{Dabco})](\text{ClO}_4)_4$ do fulfill Hoffmann's prescription⁸ for binuclear copper(II) complexes that should exhibit appreciable antiferromagnetic interactions. The Dabco complex shows no sign of an interaction down to 4.2 K and as such $|J| < \text{ca. } 0.5 \text{ cm}^{-1}$. There is a very weak antiferromagnetic interaction in the pyz compound where $J = -3.2 \text{ cm}^{-1}$. Unfortunately, the theoretical predictions are not borne out by these experimental facts. The through-bond interaction of 1–2 eV between the nitrogen lone pairs of either pyz or Dabco is apparently not sufficient to result in a strong exchange interaction between two copper(II) ions that are σ bonded.

Molecular orbital calculations of the CNDO/2 type were carried out on the pyrazine molecule in an attempt to understand this dilemma. The pyrazine molecule was assumed to have D_{2h} symmetry with the molecular dimensions given in ref 28. The magnitude of the antiferromagnetic exchange contribution to the exchange parameter J depends on the energy separation between the bonding (ϕ_1) and antibonding (ϕ_2) molecular orbitals for the binuclear complex. The two orbitals are approximated as follows:

$$\phi_1 \approx d_{z^2}^{\text{A}} + d_{z^2}^{\text{B}}$$

$$\phi_2 \approx d_{z^2}^{\text{A}} - d_{z^2}^{\text{B}}$$

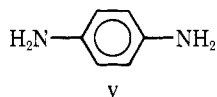
The energy separation between ϕ_1 and ϕ_2 is a consequence of the interaction of the two metal d_{z^2} orbitals, and this interaction is propagated by bridge orbitals with the appropriate symmetry. The energy of the bonding molecular orbital ϕ_1 experiences a greater change in this interaction.⁸ In the case of pyrazine there is a total of three a_g occupied bridge orbitals and the highest energy occupied a_g orbital is the one that should be the main propagator of interaction. This orbital is mainly a symmetric combination of nitrogen lone-pair orbitals as indicated in iv. It is important to note that there is a relatively



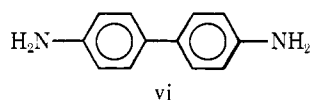
small contribution from carbon $2p_z$ orbitals in this molecular orbital. The ratio of the coefficient for the carbon orbital compared to the coefficient for the nitrogen orbital is 0.62. It seems reasonable to suggest that the weak antiferromagnetic interaction is in part due to the small contribution of carbon $2p_z$ orbitals; the bonding overlap from one Cu(II) ion to the other Cu(II) ions is not effective. Also, the low basicity of

pyrazine would lead to a Cu–N bond that is not that strong, again attenuating the antiferromagnetic interaction.

Substantiation for the above suggestions comes from the fact that the compound $[\text{Cu}_2(\text{tren})_2(\text{PPD})](\text{ClO}_4)_4$ exhibits a stronger antiferromagnetic interaction ($J = -26.2 \text{ cm}^{-1}$) than the analogous pyrazine complex.²⁹ The bridge is *p*-phenylenediamine (v). It has been deduced from CNDO/2 molecular



orbital calculations for PPD that the orbital occurring at -14.25 eV is largely responsible for propagating the metal d_{z^2} orbital interaction in this complex. This orbital is similar in composition to the highest energy occupied a_g pyrazine orbital, except that the carbon atom contributions are now comparable to the nitrogen orbital contributions (ratio of carbon to nitrogen is ca. 0.89). This may result in a more effective magnetic exchange interaction between the two Cu(II) ions. An even more surprising result is noted in the observation²⁹ that the binuclear complex $[\text{Cu}(\text{tren})_2(\text{BZD})](\text{ClO}_4)_4$, where BZD is the extended benzidine bridge vi, exhibits an antiferromagnetic in-



teraction with $J = -3.7 \text{ cm}^{-1}$. This antiferromagnetic interaction is comparable to that found for the pyrazine compound. Also, in the case of the BZD bridge, the molecular orbital occurring at -12.88 eV and assumed to be the most important orbital in propagating the exchange interaction has relatively large contributions from carbon $2p$ σ -type orbitals. It is relevant to mention here that both PPD and BZD are stronger bases than pyrazine which would impart a greater metal d_{z^2} -nitrogen orbital overlap.

The same arguments explain why $[\text{Cu}_2(\text{tren})_2(4,4'\text{-bpy})](\text{BPh}_4)_4$ does not show any signs of a magnetic exchange interaction in the susceptibility data down to 4.2 K. Moreover, its Q-band EPR spectrum is a typical trigonal bipyramidal axial spectrum with $g_{\perp} = 2.571$ and $g_{\parallel} = 2.017$. The spectrum does not exhibit any discernible hyperfine pattern that could be attributed to electron delocalization over two Cu(II) centers. The compound was isolated as a BPh_4^- salt to obtain a magnetically dilute environment for the binuclear complex. Eliminating or reducing the intermolecular dipolar and exchange interactions with a large counterion can lead to the resolution of Cu(II) hyperfine structure and other features in the EPR spectra.

The compound $[\text{Cu}_2(\text{tren})_2(\text{BPE})](\text{BPh}_4)_4$ exhibits a seven-line hyperfine pattern with an average spacing of 68 G on its g_{\parallel} signal in the Q-band EPR spectrum. The appearance of the seven-line hyperfine pattern indicates a coupling of electron spin with two equivalent Cu(II) centers. This shows that the bridge BPE can propagate a weak antiferromagnetic exchange interaction ($|J| \leq \text{ca. } 0.02 \text{ cm}^{-1}$). This conclusion cannot be overemphasized, however, because copper hyperfine patterns for trigonal bipyramidal copper(II) species have not been well characterized. Three publications have appeared in the literature³⁰⁻³² dealing with EPR spectra of five-coordinated trigonal bipyramidal copper(II) complexes. The complex $[\text{Cu}(\text{tren})\text{OH}]^+$ has been characterized to have $A_{\parallel} = 68 \text{ G}$ and $A_{\perp} = 111 \text{ G}$. An average $A = 105 \text{ G}$ has been observed for the systems studied. In an effort to obtain more insight into the problem, $[\text{Cu}_2(\text{tren})(\text{ImH})](\text{BPh}_4)_3 \cdot \text{H}_2\text{O}$ was prepared, where ImH is imidazole. The Q-band spectrum is rhombic with three g values, indicating a nonaxial coordination geometry for the copper(II) ion. Two sets of four-line copper hyperfine patterns appear, one impressed on each of the g_1 and g_2 signals with

spacings of 140 and 70 G, respectively. The $g_3(g_{\parallel})$ signal shows bumps that could be due to a hyperfine pattern, but the pattern was not well resolved. The seven-line copper hyperfine pattern on the g_1 signal for $[\text{Cu}_2(\text{tren})_2(\text{BPE})](\text{BPh}_4)_4$ has an average spacing of 68 G and this is almost half the spacing observed for the g_1 signal of the imidazole monomer. The BPE compound shows signs of slow decomposition into a yellow-brown solid with time, but the seven-line hyperfine pattern and the spectrum are still reproducible for a partially decomposed sample. In short, the seven-line copper hyperfine pattern on the g_1 signal does seem to point to the presence of a magnetic exchange interaction in $[\text{Cu}_2(\text{tren})_2(\text{BPE})](\text{BPh}_4)_4$.

While the theoretical analysis of Hoffmann et al.⁸ predicts a substantial magnetic interaction to be propagated by Dabco, the experimental magnetic susceptibility data for $[\text{Cu}_2(\text{tren})_2(\text{Dabco})](\text{ClO}_4)_4$ do not show any sign of exchange interaction down to 4.2 K. Figure 1 (tracing A) shows that μ_{eff} does not vary with temperature. Dabco has a σ framework only and in this complex it is bridging between two Cu(II) centers with σ -type d_{z^2} ground states. Because the Dabco binuclear complex does not show a measurable J as compared to the pyrazine compound, it is possible that the π system in the pyrazine ring does affect the magnitude of antiferromagnetic interaction in an indirect fashion. The importance of the pathway in the pyrazine-bridged system has been indicated previously for the polymer $\text{Cu}(\text{NO}_3)_2\text{pyz}$.⁷ Pyrazine-bridged vanadyl complexes were prepared to investigate this possibility.

The compounds $[\text{VO}(\text{hfac})_2]_2(\text{Dabco})$ and $[\text{VO}(\text{acac})_2]_2(\text{BPE})$ do not show any signs of an interaction in their susceptibility data. Figure 1 (tracing B) shows that for the Dabco compound the magnetic moment stays essentially constant down to 4.2 K. In contrast to the Cu-tren system, the vanadyl complexes have a π -type d_{xy} ground state. Therefore, Dabco, which lacks a π system, does not have a viable superexchange pathway. The same conclusion was recently reached for the polymeric compound $[\text{Cu}(\text{hfac})_2]_2\text{Dabco}$.⁵ For the BPE complex the large separation between the two V(IV) centers is most probably the main reason for the attenuation of any magnetic exchange interaction.

The susceptibility data for all three compounds with the composition $[\text{VO}(\text{hfac})_2]_2(\text{B})$, where B is pyz, 2-Me-pyz, or 2,5-Me₂-pyz, indicate an antiferromagnetic coupling and, as summarized in Table XII, the three complexes have J values of -19 , -6.7 , and -4.0 cm^{-1} , respectively. The antiferromagnetic interaction for the pyrazine-bridged vanadyl system is somewhat greater than that observed for $[\text{Cu}_2(\text{tren})_2(\text{pyz})](\text{ClO}_4)_4$. This indicates that the pyrazine orbitals are more favorably situated to overlap with a d_{xy} π -type ground state than with a d_{z^2} σ type. The decrease in antiferromagnetic interaction in $[\text{VO}(\text{hfac})_2]_2\text{B}$ as B is changed from pyz to 2-Me-pyz and finally to 2,5-Me₂-pyz could give some insight into the exchange mechanism (vide infra).

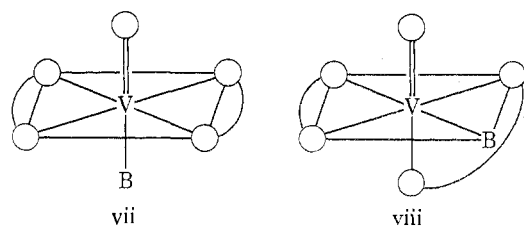
The EPR spectra of powdered samples of the vanadyl compounds are typical in that they are comprised generally of single derivatives around $g = 1.99$. The X-band spectra of $[\text{VO}(\text{hfac})_2]_2(\text{B})$, where B is 2-Me-pyz or 2,5-Me₂-pyz, taken at 10 K, show a 15-line vanadium hyperfine pattern on the g_{\parallel} signal, which clearly establishes the intramolecular nature of the antiferromagnetic interaction in these complexes. The spectrum of the 2,5-Me₂-pyz compound is shown in Figure 8.

The bridge B in the $[\text{VO}(\text{hfac})_2]_2\text{B}$ complexes can be coordinated in either an axial or equatorial site at each vanadyl ion, viz., vii and viii. This leads to three possible geometries for the $[\text{VO}(\text{hfac})_2]_2\text{B}$ complexes. In one, B bridges from an axial site to another axial site. In the second, the bridging is from equatorial site to equatorial site. The third possibility, where the bridging is from an axial site to an equatorial site, seems

Table XII. Magnetic Exchange Least-Squares Parameters

compd	J, cm^{-1}	g
$[\text{Cu}_2(\text{tren})_2(\text{pyz})](\text{ClO}_4)_4$	-3.2	2.222 ^a
$[\text{Cu}_2(\text{tren})_2(\text{PPD})](\text{ClO}_4)_4$	-26.2 ^b	
$[\text{Cu}_2(\text{tren})_2(\text{BZD})](\text{ClO}_4)_4$	-3.7 ^b	
$[\text{Cu}_2(\text{tren})_2(\text{Dabco})](\text{ClO}_4)_4$	< ca. 0.5 ^c	
$[\text{Cu}_2(\text{tren})_2(4,4'\text{-bpy})](\text{BPh}_4)_4$	< ca. 0.5 ^c	
$[\text{Cu}_2(\text{tren})_2(\text{BPE})](\text{BPh}_4)_4$	< ca. 0.5 ^c	
$[\text{Ru}(\text{NH}_3)_5(\text{pyz})](\text{OTf})_6$	< ca. 0.5 ^{c,d}	
$[\text{Cu}(\text{hfac})_2](\text{pyz})$	< ca. 0.5 ^c	
$[\text{VO}(\text{hfac})_2]_2(\text{pyz})$	-19	1.917 ^a
$[\text{VO}(\text{hfac})_2]_2(2\text{-Me-pyz})$	-6.7	1.992 ^a
$[\text{VO}(\text{hfac})_2]_2(2,5\text{-Me}_2\text{-pyz})$	-4.0	1.927 ^a
$[\text{VO}(\text{hfac})_2]_2(\text{PPD})$	< ca. 0.5 ^c	
$[\text{VO}(\text{hfac})_2]_2(\text{BPE})$	< ca. 0.5 ^c	
$[\text{Cu}(\text{pyz})_2](\text{ClO}_4)_2$	-10.8, ^g -10.1 ^g	2.060 ^e

^a In the least-squares fitting, g was varied. ^b See ref 29. The abbreviations BZD and PPD stand for benzidine and *p*-phenylenediamine, respectively. ^c In these cases there are no signs of an exchange interaction in the susceptibility data taken down to 4.2 K and, as such, $J < 0.5 \text{ cm}^{-1}$. ^d See ref 4. ^e In the least-squares fitting, this f was held fixed. ^f The parameter J was obtained by least-squares fitting to eq 1. ^g The parameter J was obtained by least-squares fitting to eq 2.



quite unlikely. The question of which structure is present is very crucial for the analysis of potential magnetic exchange pathways. X-ray powder diffraction patterns are sometimes helpful in comparative structural analyses. Consequently, X-ray diffraction patterns were obtained for the vanadyl compounds as well as for $[\text{Cu}(\text{hfac})_2]_2(\text{pyz})$, the crystal structure of which is known.⁶ The powder patterns of the compounds $[\text{VO}(\text{hfac})_2]_2\text{B}$, where B is pyz, 2-Me-pyz, or 2,5-Me₂pyz, were found to be very similar but they are different from the powder pattern that was obtained for $[\text{Cu}(\text{hfac})_2]_2(\text{pyz})$. In the latter compound the pyrazine is axial. Therefore, it is possible that the vanadyl compounds have the pyrazine moiety in an equatorial coordination position leading to a different powder pattern. At least, it can be said that the three vanadyl compounds are isostructural. As it turns out (vide infra), the analysis of the possible effective antiferromagnetic exchange pathways is more compatible with equatorial bridging of the pyrazine moiety in the vanadyl complexes.

Because the vanadyl ions have d_{xy} ground states, the exchange pathway must involve the π system of the pyrazine molecule to first order. The two highest occupied π orbitals on pyrazine are $\pi(b_{1g})$ and $\pi(b_{2g})$. The former is predominantly comprised of carbon orbitals, while the latter is mainly nitrogen orbital in composition. The $\pi(b_{1g})$ orbital is of the correct symmetry to overlap with the d_{xy} orbital of V(IV) if the pyrazine bridges axially. The $\pi(b_{2g})$ orbital is favorable for overlap with the d_{xy} orbital if the pyrazine molecule bridges from one equatorial site to another. However, the $d_{xy}-\pi(b_{1g})$ overlap is not very effective owing to the predominantly carbon orbital composition of this pyrazine orbital. In the $d_{xy}-\pi(b_{2g})$ case, the most effective metal-pyrazine overlap occurs when there is a nonzero dihedral angle between the plane of the pyrazine and the equatorial planes of the two complexes. Similar arguments have been employed by Hatfield et al.⁷ when discussing the superexchange pathway in $\text{Cu}(\text{NO}_3)_2 \cdot \text{pyz}$. Therefore, it is concluded that an equatorial bridging of the pyrazine molecule could explain the observation of appreciable antiferromagnetic interaction in $[\text{VO}(\text{hfac})_2]_2(\text{pyz})$. The decrease in the antiferromagnetic interaction as pyz is changed

to 2-Me-pyz and then 2,5-Me-pyz can be attributed to the steric interaction of the methyl groups with the hfac ligands. This could lead to a lengthening of the V-N bonds and, consequently, a weakening of the effective overlap between metal and bridge orbitals.

Finally, it should be noted that the pyrazine-bridged Ru(III) complex $[(\text{NH}_3)_5\text{-Ru-pyz-Ru}(\text{NH}_3)_5](\text{OTf})_6$ has also been reported to show no signs of a magnetic exchange interaction in susceptibility data taken down to 4.2 K.⁴ This was ascribed to a poor overlap between the low-spin d^5 ground-state orbital set (d_{xz} , d_{yz}) and the π systems of the pyrazine. In this case, the poor overlap results from the fact that the pyrazine plane is located along the z axis and bisects the N-Ru-N bond angle.

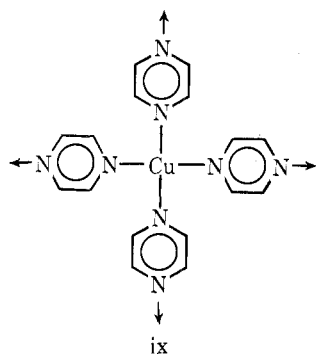
Equilibria Studies of Vanadyl Complexes. Solution equilibrium studies were carried out to aid in the interpretation of the solution EPR results. The values of K_1 and K_2 obtained indicate that for a solution which is initially $1 \times 10^{-3} \text{ M}$ in B and $2 \times 10^{-3} \text{ M}$ in A, the concentrations of A_2B , AB, and A are each $5 \times 10^{-4} \text{ M}$ in CH_2Cl_2 at room temperature. Even in a frozen toluene glass, the EPR spectrum of $[\text{VO}(\text{hfac})_2]_2\text{pyz}$ contained several resonances from monomeric vanadyl species. Thus, characterization of the complex and of the related methyl-substituted pyrazine-bridged complexes by EPR was not pursued further in the solution phase, even though a fair degree of solubility was obtained for these neutral complexes.

The equilibrium constants for formation of the 1:1 and 2:1 adducts of $\text{VO}(\text{hfac})_2$ with pyrazine indicate that coordination to one end makes a significant electronic perturbation on the second nitrogen. Statistical considerations would predict that for a noninteracting system the K_2 would be one-fourth the first K_1 . A decrease of nearly three orders of magnitude is observed. This behavior is to be contrasted to the reported increase in the value of K_2 relative to K_1 when the $\text{Ru}(\text{NH}_3)_5^{2+}$ moiety is coordinated to pyrazine.³³ The interpretation of the $\text{Ru}(\text{NH}_3)_5^{3+}$ result is somewhat obscured by potential solvent complications, for the measurements were carried out in water. However, the increase in K_2 relative to K_1 has been explained by invoking significant amounts of π back-bonding from the ruthenium center into molecular orbitals on the pyrazine. Since the electronic configuration of pseudooctahedral VO^{2+} is t_{2g}^3 , the observed decrease in K_2 relative to K_1 is due to an inductive withdrawal of electron density from the pyrazine moiety by the axial vanadyl center without the compensating π back-donation effect apparently observed in the ruthenium system.

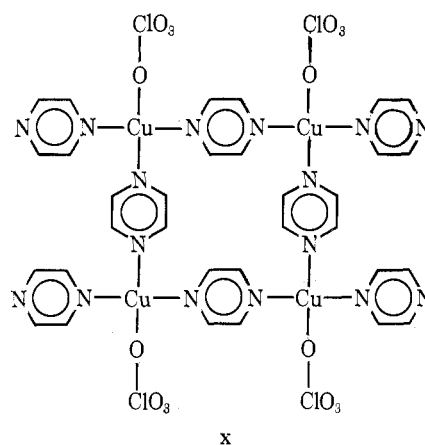
The battery of measurements carried out on these systems emphasizes a very important aspect of metallomer chemistry. The magnetic and EPR studies indicate relatively little interaction between the two metals in pyrazine-bridged dimers. These methods are very sensitive to small interactions. On the other hand, the equilibrium studies indicate that coordination of the Lewis acid $\text{VO}(\text{hfac})_2$ to one nitrogen atom of a pyrazine molecule makes a pronounced perturbation on the reactivity of the second nitrogen. The interrelationships between the magnitude of a magnetic exchange interaction in a binuclear complex as gauged by magnetism and EPR and the chemical consequences afforded by coupling two metal electronic manifolds have not been established.³⁴ Thus, it is interesting to know whether a binuclear complex with an antiferromagnetic exchange interaction of, say, $J = -100 \text{ cm}^{-1}$ in its ground state could be expected to exhibit a chemistry at each metal center that is markedly affected by the presence of the other metal center. For example, it is desirable to know the relation between the antiferromagnetic coupling in the complex and the successive one-electron reduction (oxidation) waves.

$\text{Cu}(\text{pyz})_2(\text{ClO}_4)_2$. Because the structure of this compound is least certain and because it is potentially polymeric, its properties will be described separately.

The first infrared study³⁵ of $\text{Cu}(\text{pyz})_2(\text{ClO}_4)_2$ indicated that the ClO_4^- anion is bonded through one oxygen atom. A more recent investigation⁹ of the infrared spectrum suggested that the complex most likely contains bridging pyrazine ligands. In the present study, it was found that the magnetic susceptibility data for the compound indicated an antiferromagnetic interaction. It is clear that there is a bridging species between $\text{Cu}(\text{II})$ centers. One reasonable structure for the compound is a polymeric sheet structure where every $\text{Cu}(\text{II})$ center is bonded to four pyrazine ligands. This could be represented schematically as ix. The analogous compound $\text{Co}(\text{pyz})_2\text{Cl}_2$ ³⁶



has been shown to have a sheet-type structure where all the pyrazine molecules are bridging two $\text{Co}(\text{II})$ centers. Frequently the polymeric aggregation of antiferromagnetically coupled centers leads to susceptibility curves with broad maxima. The compound $\text{Cu}(\text{pyz})_2(\text{ClO}_4)_2$, however, shows a curve with a sharp maximum at ca. 12.1 K (Figure 6). Two least-squares fittings of the data to different equations were attempted: eq 1 for a dimer and eq 2 for a tetramer where the four $\text{Cu}(\text{II})$ centers have D_{4h} symmetry. As can be seen from Figure 5, the fit to the tetramer equation is better than the fitting to the dimer equation. The J values obtained from least-squares fittings are $J(\text{dimer}) = -10.8$ and $J(\text{tetramer}) = -10.1 \text{ cm}^{-1}$. It is interesting to note that the J values are almost equal. The very good fit to the tetramer model could imply the structure x. The tetramer as well as the dimer fitting procedures were also carried out for the compound $\text{Ag}(\text{pyz})_2\text{S}_2\text{O}_8$ using the limited data set already published.³⁷ In this case, also, the tetramer fit appears to be superior to the dimer fit. The J values are $J(\text{dimer}) = -56$ and $J(\text{tetramer}) = -46 \text{ cm}^{-1}$. We could conclude that either the two compounds are actually tetramers



or the tetramer model is an approximation to the model needed for the polymeric sheet structure.

The Q-band and the X-band spectra of $\text{Cu}(\text{pyz})_2(\text{ClO}_4)_2$ are very characteristic of a square-planar copper(II) coordination geometry. Therefore, the unpaired electron is residing mainly in a $d_{x^2-y^2}$ orbital. In order for an effective propagation of exchange interaction the bridging pyrazine plane should be canted relative to the xy plane defined by the square-planar coordination geometries of the $\text{Cu}(\text{II})$ ions. This will put the $\pi(b_{1g})$ orbital of pyrazine in the best orientation for overlapping positively with the $d_{x^2-y^2}$ orbitals on the $\text{Cu}(\text{II})$ centers. This is analogous to the situation in the $\text{Cu}(\text{NO}_3)_2\text{pyz}$ polymer.⁷ In $\text{Co}(\text{pyz})_2\text{Cl}_2$,³⁷ the pyrazine rings are tilted about the N-N axes at an angle of 44.4° to the planes of the cobalt atoms. The cobalt system, however, does not show any sign of an exchange interaction down to 1.8 K.³⁸

Conclusion

It has been shown that pyrazine (and for that matter Dabco) is not a very viable bridging species to propagate magnetic exchange interactions between two paramagnetic transition metal ions. Binuclear copper(II) complexes with d_{22} ground states only show weak antiferromagnetic interactions when bridged by pyrazine. Pyrazine, thus, does not effectively support a spin-spin coupling via a σ orbital pathway. Only moderately strong antiferromagnetic interactions were found for several binuclear vanadyl complexes, implying that pyrazine does not afford an effective π -orbital exchange pathway either. In contrast to this behavior, coordination of a vanadyl complex to one of the nitrogens of pyrazine greatly reduced the coordination ability of the second nitrogen atom.

Note Added in Proof. The X-ray structure of $[\text{Cu}(\text{pyz})_2](\text{ClO}_4)_2$ has been determined. The compound has a polymeric sheet structure. Details of the structure, as well as a reevaluation of the magnetic susceptibility data, will appear in a forthcoming paper.

Acknowledgment. D.N.H. is grateful for support from National Institutes of Health Grant HL 13652. R.S.D. is grateful for support from the National Science Foundation through Grant CHE 76 20064 A01. Drs. Dennis Eberl and Hani Khoury from the Geology Department at the University of Illinois are to be thanked for their help in the X-ray diffraction work. Mr. Bruce Bunker is to be thanked for his help in the liquid helium EPR work.

Supplementary Material Available: Tables I-XI (experimental and calculated magnetic susceptibility data) (15 pages). Ordering information is given on any current masthead page.

References and Notes

- (1) University of Illinois Fellow, 1976-1979.
- (2) Camille and Henry Dreyfus Fellow, 1972-1977; A. P. Sloan Foundation

- Fellow, 1976–1978.
- (3) C. Creutz and H. Taube, *J. Am. Chem. Soc.*, **91**, 3988 (1969).
 - (4) B. C. Bunker, R. S. Drago, D. N. Hendrickson, S. L. Kessel, and R. Richman, *J. Am. Chem. Soc.*, **100**, 3805 (1978).
 - (5) H. W. Richardson, J. R. Wasson, and W. E. Hatfield, *Inorg. Chem.*, **16**, 484 (1977).
 - (6) R. C. E. Belford, D. E. Fenton, and M. E. Truter, *J. Chem. Soc., Dalton Trans.*, 17 (1974).
 - (7) H. W. Richardson and W. E. Hatfield, *J. Am. Chem. Soc.*, **98**, 835 (1976).
 - (8) P. J. Hay, J. C. Thibeault, and R. Hoffmann, *J. Am. Chem. Soc.*, **97**, 4884 (1975).
 - (9) M. K. Child and G. C. Percy, *Spectrosc. Lett.*, **10**, 71 (1977).
 - (10) C. Su, J. W. Reed, and E. S. Gould, *Inorg. Chem.*, **12**, 337 (1973).
 - (11) R. A. Rowe and M. M. Jones, *Inorg. Synth.*, **5**, 114 (1957).
 - (12) R. C. E. Belford, D. E. Fenton, and M. R. Truter, *J. Chem. Soc., Dalton Trans.*, 2208 (1972).
 - (13) T. C. Kuechler, Ph.D. Thesis, University of Illinois, 1977, p 91.
 - (14) D. M. Duggan, E. K. Barefield, and D. N. Hendrickson, *Inorg. Chem.*, **12**, 985 (1973).
 - (15) B. N. Figgis and J. Lewis in "Modern Coordination Chemistry", J. Lewis and R. G. Wilkins, Ed., Interscience, New York, N.Y., 1960, p 403.
 - (16) J. P. Chandler, Program 66, Quantum Chemistry Program Exchange, Indiana University, Bloomington, Ind., 1973.
 - (17) E. J. Laskowski, T. R. Felthouse, and D. N. Hendrickson, *Inorg. Chem.*, **16**, 1077 (1977).
 - (18) J. A. Pople and D. L. Beveridge, "Approximate Molecular Orbital Theory", McGraw-Hill, New York, N.Y., 1970.
 - (19) See paragraph at end of paper regarding supplementary material.
 - (20) B. Bleaney and K. D. Bowers, *Proc. R. Soc. London, Ser. A*, **214**, 451 (1952).
 - (21) W. E. Hatfield in "Theory and Applications of Molecular Paramagnetism", E. A. Boudreaux and L. N. Muly, Ed., Wiley, New York, N.Y., 1976, Chapter 7, p 349.
 - (22) A. P. Ginsbert, R. L. Martin, R. W. Brookes, and R. C. Sherwood, *Inorg. Chem.*, **11**, 2884 (1972).
 - (23) D. M. Duggan and D. N. Hendrickson, *Inorg. Chem.*, **13**, 1911 (1974).
 - (24) E. J. Laskowski, D. M. Duggan, and D. N. Hendrickson, *Inorg. Chem.*, **14**, 2449 (1975).
 - (25) T. R. Felthouse, E. N. Duesler, and D. N. Hendrickson, *J. Am. Chem. Soc.*, **100**, 618 (1978).
 - (26) P. C. Jain and E. C. Lingafelter, *J. Am. Chem. Soc.*, **89**, 724 (1967).
 - (27) H. Taube, "Bioinorganic Chemistry-II", *Adv. Chem. Ser.*, **No. 162** (1977).
 - (28) J. A. Merritt and K. K. Innes, *Spectrochim. Acta*, **16**, 945 (1960).
 - (29) T. R. Felthouse and D. N. Hendrickson, *Inorg. Chem.*, **17**, 2836 (1978).
 - (30) G. A. Senyukova, I. D. Mikheikin, and K. I. Zamarev, *Russ. J. Struct. Chem. (Engl. Transl.)*, **11**, 18 (1970).
 - (31) R. Barbucci and M. J. M. Campell, *Inorg. Chim. Acta*, **15**, L15 (1975).
 - (32) R. Barbucci, A. Bencini, and D. Gatteschi, *Inorg. Chem.*, **16**, 2117 (1977).
 - (33) P. Ford, De F. P. Rudd, R. Gauder, and H. Taube, *J. Am. Chem. Soc.*, **90**, 1187 (1968).
 - (34) R. S. Drago, T. C. Kuechler, and M. Kroeger, submitted for publication.
 - (35) M. Sekizaki, K. Yamasaki, and K. Hayashi, *Nippon Kagaku Zasshi*, **91**, 1191 (1970).
 - (36) P. W. Carreck, M. Goldstein, E. M. McPartlin, and W. D. Unsworth, *Chem. Commun.*, 1634 (1971).
 - (37) R. W. Matthews and R. A. Walton, *Inorg. Chem.*, **10**, 1433 (1971).
 - (38) M. Inoue and M. Kubo, *Coord. Chem. Rev.*, **21**, 1 (1976).

Preparations and Properties of Nitrosyl Complexes of Iron Tetramethylcyclam. X-ray Structures of $[\text{Fe}(\text{C}_{14}\text{H}_{32}\text{N}_4)\text{NO}](\text{BF}_4)_2$, a $S = 3/2 - 1/2$ Spin-Equilibrium Complex, and $[\text{Fe}(\text{C}_{14}\text{H}_{32}\text{N}_4)(\text{NO})(\text{OH})](\text{ClO}_4)_2 \cdot \text{CH}_3\text{CN}$

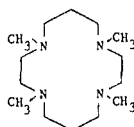
Keith D. Hodges,^{1a,b} R. G. Wollmann,^{1b} S. L. Kessel,^{1b} D. N. Hendrickson,^{*1b,c}
D. G. Van Derveer,^{1a} and E. Kent Barefield^{*1a}

Contribution from the School of Chemistry, Georgia Institute of Technology, Atlanta, Georgia 30332, and the School of Chemical Sciences, University of Illinois, Urbana, Illinois 61801. Received July 13, 1978

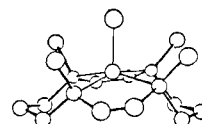
Abstract: Reactions of $[\text{Fe}(\text{TMC})(\text{NCCH}_3)](\text{BF}_4)_2$ (TMC = 1,4,8,11-tetramethyl-1,4,8,11-tetraazacyclotetradecane) with $\text{NO}(\text{g})$ in CH_3NO_2 and NOBF_4 in CH_3CN yield green, paramagnetic $[\text{Fe}(\text{TMC})\text{NO}](\text{BF}_4)_2$ and red, diamagnetic $[\text{Fe}(\text{TMC})(\text{NO})(\text{OH})](\text{BF}_4)_2 \cdot \text{CH}_3\text{CN}$, respectively. The hydroxyl group in the latter complex apparently comes from water impurities in the CH_3CN . Physical and chemical properties of these complexes are reported. Of note is the temperature-dependent magnetic moment of $[\text{Fe}(\text{TMC})\text{NO}](\text{BF}_4)_2$, which ranges from 3.62 μ_B at 286 K to 2.66 μ_B at 4.2 K. IR, EPR, and Mössbauer data support a $S = 3/2 - 1/2$ spin equilibrium for the complex. Single-crystal, X-ray structures of $[\text{Fe}(\text{TMC})\text{NO}](\text{BF}_4)_2$ and $[\text{Fe}(\text{TMC})(\text{NO})(\text{OH})](\text{ClO}_4)_2 \cdot \text{CH}_3\text{CN}$ (obtained by metathesis of the BF_4^- salt) are also described. $[\text{Fe}(\text{TMC})\text{NO}](\text{BF}_4)_2$ crystallizes in space group $P2_1/c$ with four molecules in a cell of dimensions $a = 8.658$ (5) Å, $b = 17.317$ (5) Å, $c = 15.132$ (8) Å; $\beta = 91.93$ (4)°, $\rho_{\text{calcd}} = 1.51$ g cm^{-3} , $\rho_{\text{obsd}} = 1.49$ (2) g cm^{-3} . Full-matrix least-squares refinement of 2777 reflections having $I > 3\sigma_I$ gave $R = 0.060$ and $R_w = 0.059$. The cation is five-coordinate with the nitrosyl group in the apical position of a distorted tetragonal pyramid; the Fe–N–O angle is 177.5 (5)° with Fe–NO and FeN–O interatomic distances of 1.737 (6) and 1.137 (6) Å, respectively. The electronic structure of this unusual nitrosyl complex is described by a modified $\{\text{FeNO}\}^7$ model. The hydroxy-nitrosyl complex crystallizes in space group $P\bar{1}$ with two molecules in a cell of dimensions $a = 10.823$ (4) Å, $b = 14.489$ (4) Å, $c = 14.489$ (4) Å; $\alpha = 134.61$ (2)°, $\beta = 108.97$ (2)°, $\gamma = 98.47$ (3)°, $\rho_{\text{calcd}} = 1.61$ g cm^{-3} , $\rho_{\text{obsd}} = 1.57$ (2) g cm^{-3} . Full-matrix, least-squares refinement of 3027 reflections having $I > 3\sigma_I$ gave $R = 0.067$ and $R_w = 0.064$. The cation consists of six-coordinate iron, axially coordinated by the NO and OH groups. As in the $[\text{Fe}(\text{TMC})\text{NO}]^{2+}$ cation, the axially oriented *N*-methyl groups are all on the same side of the Fe–TMC moiety as the nitrosyl group. This is the first structurally characterized six-coordinate complex of TMC having this set of nitrogen configurations. The Fe–N–O angle is 178.3 (6)° with Fe–NO and Fe–OH interatomic distances of 1.621 (6) and 1.798 (3) Å, respectively. The iron atom is 0.156 Å out of the N_4 plane toward the nitrosyl ligand.

Introduction

Macrocyclic tetramine I (1,4,8,11-tetramethyl-1,4,8,11-tetraazacyclotetradecane, abbreviated TMC)^{2a} binds metal ions in a stereospecific fashion such that the four *N*-methyl substituents lie on the same side of the metal–nitrogen plane as shown by II.^{2b} This extreme differentiation of the two sides



1



11